Nucleon polarizabilities and Δ-resonance magnetic moment in chiral EFT

Vladimir Pascalutsa

Institut für Kernphysik, Johannes Gutenberg Universität, Mainz D-55099, Germany

Abstract. Recent chiral EFT calculations of nucleon polarizabilities reveal a problem in the current empirical determination of proton's electromagnetic polarizabilities. We also report on the progress in the empirical determination of the Δ(1232)-resonance magnetic moment in the process of $\gamma p \to p\pi^0\gamma'$ measured at MAMI.

Keywords: chiral expansion, dispersion relations, electromagnetic polarizabilties, resonance magnetic moment
PACS: 14.20.Dh, 14.20.Gk, 13.60.Fz, 13.60.Le, 11.30.Rd, 11.55.Fv

1. INTRODUCTION

The chiral effective-field theory (χEFT) describes the physics of low-energy strong interaction in terms of hadronic degrees of freedom, rather than in terms of the underlying quarks and gluons. Originally χEFT dealt with only the Nambu-Goldstone bosons (pions, kaons) of the spontaneous chiral symmetry breaking [1, 2], but the lightest baryons have eventually been included too [3]. The inclusion of baryons has proved to be difficult and even until now there is no consensus on how to count the baryon contributions. However, my aim here is not to discuss the various counting schemes; this is done elsewhere [4]. I am concerned here with the question of what χEFT, combined with experiment, can tell us about the nucleon and its first excitation, the Δ(1232)-isobar.

The two sets of quantities considered here (nucleon polarizabilities and Δ's magnetic dipole moment) bear at least one thing in common: they are not measured directly but rather are extracted from experimental data using theoretical modeling. In principle the χEFT should be a suitable framework for this task, and we are going to focus on it here. The results for polarizabilities have been obtained in collaboration with Vadim Lensky [5, 6], while the work on Δ's MDM is being done together with Marc Vanderhaeghen [7, 8]. In both cases I will present here some new, thusfar unpublished results.

2. COMPTON SCATTERING: NUCLEON POLARIZABILITIES

Proton's electric (α) and magnetic (β) polarizabilities are determined in low-energy Compton scattering ($\gamma p \to \gamma p$). The purely elastic process is described by Born contributions which give rise to the Powell cross section. Polarizabilities are characterized by the inelastic contribution. At the level of unpolarized differential cross section we have:

$$\frac{d\sigma}{d\Omega} - \frac{d\sigma^{(\mathrm{Born})}}{d\Omega} = -\frac{e^2}{8\pi M_p}\left(\frac{\nu'}{\nu}\right)^2 \nu\nu' \times \Big[(\alpha+\beta)(1+z)^2 + (\alpha-\beta)(1-z)^2\Big] + O(\nu^3), \quad (1)$$

where e and M_p are the proton charge and mass, ν (ν') is the incoming (outgoing) photon energy in the lab system, z is the cosine of the lab scattering angle, $d\Omega = 2\pi\, dz$. This is a model-independent result and the Born term is known, hence by measuring the angular distribution at very low energy one should be able to determine α and β.

However, the experiments at low energies are very tough. So far most of the data are obtained for energies above 100 MeV, where the low-energy expansion begins to diverge, due to proximity of the pion production cut which sets the convergence radius. The last and the best —in terms of statistics and coverage— experiment, performed by the A2/TAPS Collaboration at MAMI [9], employed a dispersion-relation (DR) model of L'vov [10] to extract α and β. The result of this extraction is displayed in Fig. 1 by a dashed ellipse labeled 'TAPS'. Applying the Baldin sum rule value for the sum of polarizabilities cuts out the 'global average' result which is quoted by the Particle Data Group [11], namely :

$$\text{PDG:} \qquad \alpha = (12.0 \pm 0.6)\times 10^{-4}\,\mathrm{fm}^3, \quad \beta = (1.9 \pm 0.5)\times 10^{-4}\,\mathrm{fm}^3. \quad (2)$$

What is remarkable is that the present χEFT calculations [6, 12] differ from PDG in the values for polarizabilities (see the red and the grey blobs) while agreeing with the cross-section data. For instance, the next-to-next-to-leading order (NNLO) calculation in baryon

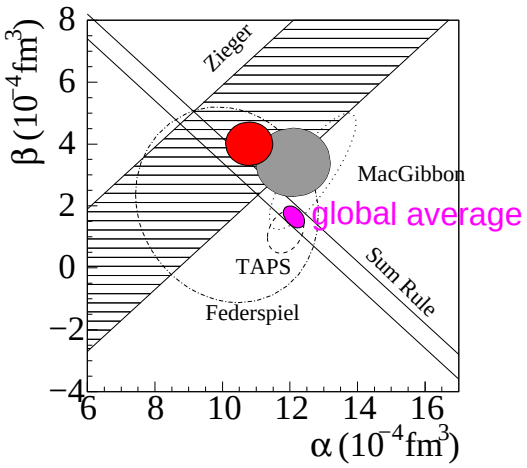

FIGURE 1. The NNLO BChPT result [6] is shown by the red blob and the Δ-less HBχPT result [12] is shown by the grey blob. 'Sum Rule' indicates the Baldin sum rule constraint on $\alpha+\beta$. Experimental results are from Federspiel et al. [13], Zieger et al. [14], MacGibbon et al. [15], and TAPS [9]. 'Global average' represents the PDG summary [11].

chiral perturbation theory (BχPT) yields [6]:

$$\begin{aligned} \text{B}\chi\text{PT}: \qquad & \alpha = (10.8 \pm 0.7) \times 10^{-4}\ \text{fm}^3, \\ & \beta = (4.0 \pm 0.7) \times 10^{-4}\ \text{fm}^3, \end{aligned} \tag{3}$$

and at the same time gives the red solid curves for the cross section in Fig. 2. The cyan-colored band around these curves corresponds to uncertainty of $\pm 0.7 \times 10^{-4}$ fm^3 in both α and β, which is exactly the radius of the red blob in Fig. 1. The DR code of L'vov produces the dotted black curves for the same values of α and β, and the dashed blue curves for the PDG values given in Eq. (2). The TAPS data are shown by black dots. The other data are properly referenced in [6].

The figure shows that for the same values of α and β the DR and χEFT yield nearly the same results. Thus, the observed discrepancy between the χEFT and PDG results is not because of the difference in theoretical approaches—they agree where they should, but because the extraction from the TAPS data went bad apparently, at least in the error estimate. One can see with a bare eye that the cross-section data do not prefer the blue-dashed curves (PDG value) over the black-dotted curves (BχPT value) to any significance. In fact, at backward angles the BχPT curves are even in a better agreement with the data.

It is fair to conclude that the existing cross-section data do not corroborate the claimed accuracy of proton polarizabilities. This is quite unfortunate because we do need a precise knowledge of these quantities, whether it is to understand the atomic measurements or to provide a basis for determinations of proton's spin polarizabilities. A

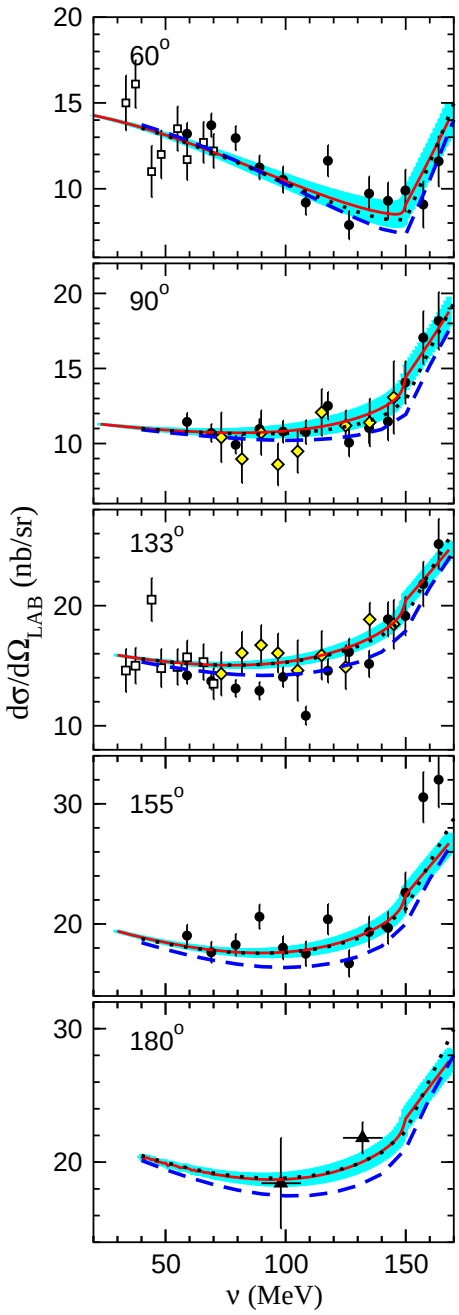

FIGURE 2. Energy dependence of $\gamma p \to \gamma p$ differential cross section, at fixed scattering angles. The curves are explained in the text.

new accurate measurement of Compton scattering below pion-production threshold can of course remedy this situation. It would be particularly interesting to use polarized beam, as proposed at the HIγS facility [16]. The polarized beam allows one to separate α and β, which is very important since the smallness of β makes it difficult for

observation in the α-dominated unpolarized cross section. We have checked that the cross sections for the photon beam linearly polarized in the scattering plane ($||$) or orthogonal to it ($\perp$) have the following expression at leading order in the low-energy expansion:

$$\begin{aligned}\frac{d\sigma_{||}}{d\Omega}-\frac{d\sigma_{||}}{d\Omega}^{(\mathrm{Born})}&=-\frac{e^2}{2\pi M_p}\left(\frac{v'}{v}\right)^2 vv'(\alpha z^2+\beta z),\\ \frac{d\sigma_{\perp}}{d\Omega}-\frac{d\sigma_{\perp}}{d\Omega}^{(\mathrm{Born})}&=-\frac{e^2}{2\pi M_p}\left(\frac{v'}{v}\right)^2 vv'(\alpha+\beta z),\end{aligned} \tag{4}$$

and hence by measuring these cross sections one would be able to determine α and β independently.

3. RADIATIVE PION PHOTOPRODUCTION: Δ'S MDM

Recent measurement of the radiative pion photoproduction ($\gamma p \to p\pi^0\gamma'$) [17] aimed at a determination of the $\Delta(1232)$-resonance magnetic dipole moment (MDM). The obtained data, however, could not be well-described using the existing theoretical frameworks, including a χEFT calculation [7, 8]. Any extraction then becomes a moot point.

It is now better understood what the problem is. A large portion of the data lies outside the Δ-resonance region. This is best seen in by plotting the data as function of the incoming photon energy, see Fig. 3, rather than as function of outgoing photon energy as it's usually done. The red/black data points in this figure are from the dedicated experiment [17], while the green/brown points are from a preliminary analysis of newer data [18].

The χEFT calculation clearly shows the resonant structure but the data-binning is so wide that one cannot distinguish it. Of course, a comparison of theory with the data below or above the resonance should be applied with caution since at least the χEFT calculation cannot be applied at arbitrary energies. The present calculation [8] is done at a next-to-leading order in the resonance regime of the δ-counting scheme [19, 20], and as such works only in a narrow window around the resonance. This can be seen, e.g., from Fig. 4 where the corresponding description of pion-photoproduction observables is shown in the region of 50 MeV around the resonance.

The Fig. 3 also shows that the differential cross section is largely insensitive to the value of Δ^+ MDM. In fact, the dependence of this observable on the MDM is quadratic, i.e., an expansion of in powers of the outgoing photon energy (E'_γ) can be written as:

$$E'_\gamma\, d\sigma/dE'_\gamma = s_0 + s_1 E'_\gamma + s_2 \mu_\Delta^2 E'^2_\gamma + O(E'^3_\gamma), \tag{5}$$

where real-valued s_i depend on the mass, width, charge and spin of the resonance, but are independent of its magnetic moment.

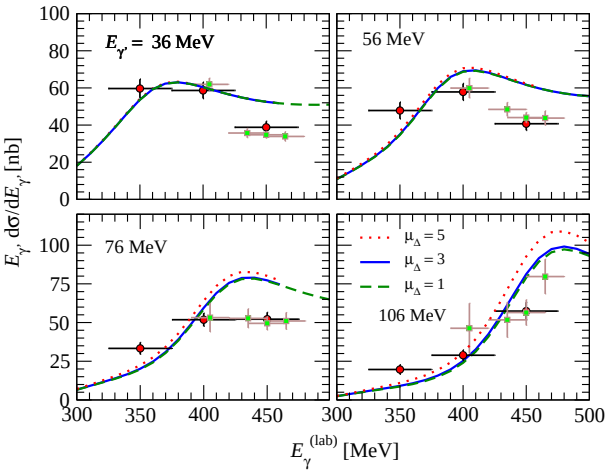

FIGURE 3. Differential cross section of $\gamma p \to p\pi^0\gamma'$ as function of photon beam energy. The curves are results of χEFT calculation [8] for different values of the Δ MDM (in units of nuclear magneton). The data points are from Crystal Ball @MAMI Collaboration: red—[17], green—[18].

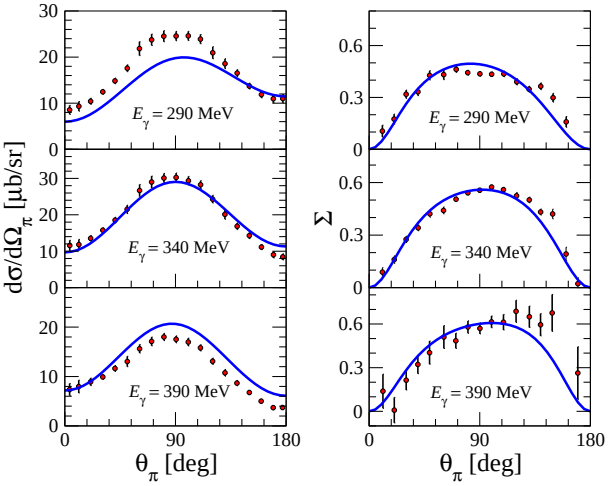

FIGURE 4. Differential cross-section and beam asymmetry of $\gamma p \to p\pi^0$ in NLO χEFT [8, 20].

It is much easier and more feasible to extract the MDM from a linearly-dependent quantity. One example of such an observable is a circularly-polarized photon beam asymmetry defined in [8]. Unfortunately this asymmetry is very small and tough to measure. Unpolarized observables of this kind are therefore welcome.

We propose an asymmetry of the outgoing pion and photon landing into different forward/backward hemispheres versus landing the same forward/backward hemisphere. In terms of the 5-fold differential cross section in the center-of-mass system this asymmetry is de-

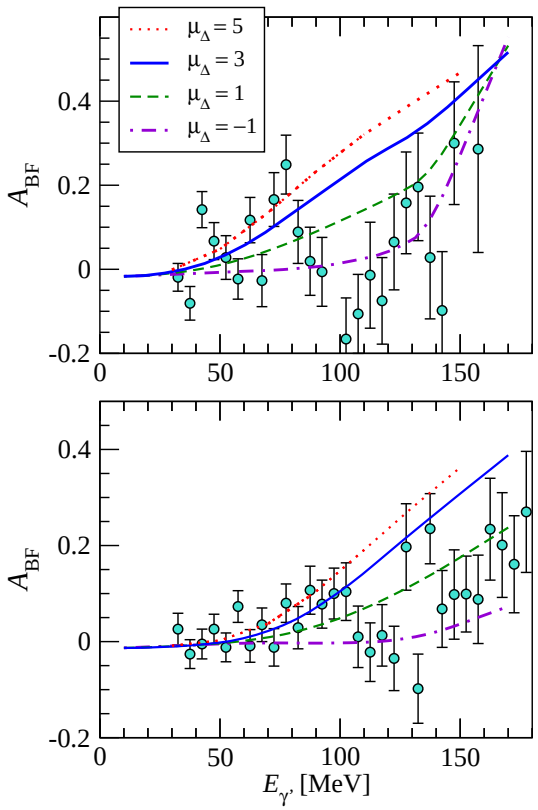

FIGURE 5. Backward-forward asymmetry for different values of the Δ MDM, at fixed beam energy: 350 MeV – upper panel, 400 MeV – lower panel, as a function of outgoing photon energy. Data points are from a preliminary analysis of CB@MAMI Collaboration [21].

fined as:

$$A_{BF} = \frac{1}{d\sigma/dE'_\gamma}\Big[\int_0^{\frac{\pi}{2}} d\Omega_{\gamma'}\int_{\frac{\pi}{2}}^{\pi} d\Omega_\pi + \int_{\frac{\pi}{2}}^{\pi} d\Omega_{\gamma'}\int_0^{\frac{\pi}{2}} d\Omega_\pi - \int_0^{\frac{\pi}{2}} d\Omega_{\gamma'}\int_0^{\frac{\pi}{2}} d\Omega_\pi - \int_{\frac{\pi}{2}}^{\pi} d\Omega_{\gamma'}\int_{\frac{\pi}{2}}^{\pi} d\Omega_\pi\Big]\frac{d^5\sigma}{dE'_\gamma d\Omega_{\gamma'} d\Omega_\pi}. \quad (6)$$

Its low-energy expansion goes as

$$A_{BF} = a_0 + a_1\,\mu_\Delta E'_\gamma + O(E'^2_\gamma), \quad (7)$$

and thus the MDM becomes seen at lower energy. Some χEFT results for this asymmetry are shown in Fig. 5, and can be compared to a preliminary analysis using the database of the dedicated CB@MAMI experiment [17]. One can see a significant sensitivity of this asymmetry on the MDM value. However, the present data are neither accurate nor consistent enough to determine the Δ^+ MDM with any good precision.

4. CONCLUSION

The existing data on proton Compton scattering cross-sections do not corroborate the claimed (e.g., in PDG tables) precision of our knowledge of proton's electric and magnetic polarizabilities. New experiments, using polarized photon beam, are needed to correct this situation.

A reliable extraction of the Δ-resonance magnetic dipole moment from the process of radiative pion production will require a substantial improvement in the experimental database, as well as further systematic refinements of the theoretical modeling.

ACKNOWLEDGMENTS

I am indebted to Jürgen Ahrens for providing me with the results of L'vov's dispersion relations shown in Fig. 2.

REFERENCES

1. S. Weinberg, Physica A **96**, 327 (1979).
2. J. Gasser and H. Leutwyler, Annals Phys. **158** (1984) 142.
3. J. Gasser, M. E. Sainio and A. Svarc, Nucl. Phys. B **307**, 779 (1988).
4. V. Pascalutsa, "Baryon Chiral Perturbation Theory: An Update," plenary talk at BARYONS'10, Osaka, Japan, Dec. 7-11, 2010.
5. V. Lensky and V. Pascalutsa, Pisma Zh. Eksp. Teor. Fiz. **89**, 127 (2009) [JETP Lett. **89**, 108 (2009)].
6. V. Lensky and V. Pascalutsa, Eur. Phys. J. C **65**, 195 (2010).
7. V. Pascalutsa and M. Vanderhaeghen, Phys. Rev. Lett. **94**, 102003 (2005).
8. V. Pascalutsa and M. Vanderhaeghen, Phys. Rev. D **77**, 014027 (2008).
9. V. Olmos de Leon *et al.*, Eur. Phys. J. A **10**, 207 (2001).
10. A. I. L'vov, Sov. J. Nucl. Phys. **34**, 597 (1981) [Yad. Fiz. **34**, 1075 (1981)].
11. K. Nakamura *et al.* [Particle Data Group], J. Phys. G **37**, 075021 (2010).
12. S. R. Beane, M. Malheiro, J. A. McGovern, D. R. Phillips and U. van Kolck, Phys. Lett. B **567**, 200 (2003) [Erratum-ibid. B **607**, 320 (2005)]; Nucl. Phys. A **747**, 311 (2005).
13. F. J. Federspiel *et al.*, Phys. Rev. Lett. **67**, 1511 (1991).
14. A. Zieger *et al.*, Phys. Lett. B **278**, 34 (1992).
15. B. E. MacGibbon *et al.*, Phys. Rev. C **52**, 2097 (1995).
16. M. W. Ahmed, talk at INT Workshop "Soft Photons and Light Nuclei," Seattle, June 16 - 20, 2008.
17. S. Schumann *et al.*, Eur. Phys. J. A **43**, 269 (2010).
18. Sergey Prakhov, private communication (May 2010).
19. V. Pascalutsa and D. R. Phillips, Phys. Rev. C **67**, 055202 (2003).
20. V. Pascalutsa, M. Vanderhaeghen and S. N. Yang, Phys. Rept. **437**, 125 (2007).
21. Sven Schumann, private communication (March 2010).